ADVANCED MATERIALS
www.advmat.de

Synthesis of Multiaryl-Substituted Pyridine Derivatives and Applications in Non-Doped Deep-Blue OLEDs as Electron-Transporting Layer with High Hole-Blocking Ability

By *Na Li, Pengfei Wang,* Shiu-Lun Lai, Weimin Liu, Chun-Sing Lee,**
Shuit-Tong Lee, and *Zengtao Liu*

In recent years, increasing demands for full-color flat-panel displays have accelerated the development of different display technologies. Among these, organic light-emitting devices (OLEDs) have attracted much attention since the report by Tang and Vanslyke[1] for their promising applications. Much effort has been made to improve the performance of OLEDs from many aspects. For example, new materials have been designed, synthesized, and applied in OLEDs. In comparison with the development of many high-performance light-emitting materials (LEMs) and hole-transporting materials (HTMs), there are relatively few reports on good electron-transporting materials (ETMs).[2–4] After three decades of research since Tang and Vanslyke's work,[1] tris(8-hydroxyquinoline)aluminum (Alq_3) is still one of the most widely used ETMs even though its electron drift mobility is more than one order lower than the hole drift mobility of typical HTMs.[5–7] In addition, another traditional hole-blocking material is often required for use with Alq_3 to improve electron charge balance, because of its poor hole-blocking ability. This would inevitably increase the device fabrication complexity. For some applications, such as in phosphorescent OLEDs or other OLEDs with hosts for light-emitting dopants, a good hole-blocking ability is an important additional requirement for the ETMs in order to simplify the device fabrication.[8,9] Materials that can fulfil these requirements are so far limited. 1,3,5-Tris(phenyl-2-benzimidazolyl)benzene (TPBI) is one such material with good electron-transporting properties and hole-blocking properties. Unfortunately, TPBI molecules in an amorphous film tend to crystallize and can lead to stability problems.[10] 4,7-Diphenyl-1,10-phenanthroline (BPhen) is another commonly used ETM that does have a good hole-blocking ability. However, its potential for commercial applications is again low because of its poor stability. Thus, it is important to explore ETMs with excellent electron-transporting and hole-blocking properties and good thermal stability. Indeed, extensive efforts have been made to increase the highest occupied molecular orbital (HOMO) energies of materials to enhance their hole-blocking ability. For example, Suzuki et al. reported a series of perfluorinated phenylene dendrimers with electron-transporting properties and large HOMO values in the early 20th century.[11] Su and Kido have recently reported several ETMs with hole-blocking ability.[12–14] However, an increase in the value of the HOMO is often accompanied by a decrease in the value of the lowest unoccupied molecular orbital (LUMO). Inevitably, smaller LUMO values, which can increase the barrier between the cathode and ETMs, suggest that electron injection from the cathode to the ETMs would become more difficult. However, herein, two multiaryl-substituted pyridine derivatives have been designed and synthesized to have large HOMO and LUMO values (i.e., energy levels are pulled down as a whole in the electron energy diagram). It is thus a challenge to synthesize such materials from the point of view of molecular design.

In this work, two novel multiaryl-substituted pyridine derivatives, namely 4,4′-(1,4-phenylene) bis(2-phenyl-6-*p*-tolylnicotinonitrile) (p-PPtNT) and 6,6′-(1,4-phenylene) bis(2-phenyl-4-*p*-tolylnicotinonitrile) (p-PPtNN) were synthesized and applied as ETMs with good hole-blocking properties. They were found to have suitable LUMO values (>3.50 eV) to allow efficient electron injection. They also have HOMO values as large as 6.87 eV, which are among the highest reported for molecular semiconductor materials.[12–14] By introducing a methyl group, adverse effects because of molecular aggregation and crystallization can be effectively avoided. Furthermore, the new materials do show good electron-transporting and hole-blocking abilities. These properties facilitate their applications as electron-transporting hosts in high-performance OLEDs.

Two multiaryl-substituted pyridine derivatives, p-PPtNT and p-PPtNN, are reported here. Synthetic routes and molecular structures are shown in Scheme 1. The two pyridine derivatives were synthesized as described in the literature.[15–17] They were synthesized by cyclocondensation of p-PPtNT I and p-PPtNN I with benzoylacetonitrile in the presence of ammonium acetate, respectively, and their spectroscopic and thermal data are listed in Table 1. From Table 1 they are found to have relatively high

---

[*] Prof. P. Wang, Dr. N. Li, Dr. W. Liu
Key Laboratory of Photochemical Conversion and Optoelectronic Materials
Technical Institute of Physics and Chemistry
Chinese Academy of Sciences
Beijing, 100190 (P. R. China)
E-mail: wangpf@mail.ipc.ac.cn

Prof. C.-S. Lee, Prof. S.-T. Lee, Dr. S.-L. Lai, Dr. Z. Liu
Center of Super-Diamond and Advanced Films (COSDAF)
Department of Physics and Materials Science
City University of Hong Kong, Hong Kong SAR (P. R. China)
E-mail: apcslee@cityu.edu.hk

DOI: 10.1002/adma.200902430

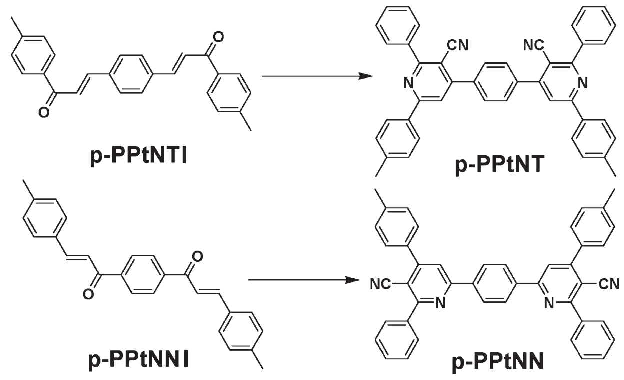

Scheme 1. The molecular structures and synthetic route of the two pyridine compounds.

glass-transition temperatures (T_gs) (138.5 °C for p-PPtNT, 101.5 °C for p-PPtNN), because of the methyl group introduced to the molecules, in comparison with that (60 °C) of BPhen. Films of the new compounds should thus have good thermal stability against crystallization. It is also noted from Table 1 that the LUMO value for p-PPtNT is 3.57 eV, while that for p-PPtNN is 3.69 eV. As is well known, the LUMO values for traditional ETMs, such as Alq_3, TPBI, and BPhen, are all lower than 3.0 eV (i.e., the energy levels are higher).[18–20] It is more difficult for electrons to inject from the cathode to the ETMs, because of the large barrier (>0.7 eV) between the cathode (the energy level of the MgAg alloy is 3.70 eV) and ETM. Therefore, the lower LUMO energy levels for the two pyridine derivatives, which imply no barrier, facilitate electron injection from the cathode to the organic layer. p-PPtNT and p-PPtNN have HOMO values (6.81 and 6.87 eV, respectively) higher than those of BCP (6.7 eV),[18] TPBI (6.7 eV),[19] and BPhen (6.4 eV).[20] These imply that the compounds can be used as hole blockers. From Table 1, it can be found that the HOMO and the LOMO values of p-PPtNN are a little larger than those of p-PPtNT. It is considered that the sp-hybrid cyano group in the *para*-orientation in p-PPtNN has a higher electron withdrawing ability and thus lowers the energy levels. This is also the reason for the red shift of the absorption and the emission peaks of p-PPtNN (λ^{ab}_{max}: 290/355 nm; λ^{em}_{max}: 427 nm) in contrast with those of p-PPtNT in the solid film (λ^{ab}_{max}: 294/330 nm; λ^{em}_{max}: 407 nm). The triplet energy (E_T) values of p-PPtNT and p-PPtNN are 3.04 and 2.99 eV, respectively (Table 1). The values are higher than a typical phosphorescent emitter, such as iridium(III) bis[(4,6-difluorophenyl)-pyridinato-*N*,C2′] picolinate (FIrpic, 2.65 eV) and fac-tris(2-phenylpyridine) iridium ($Ir(PPy)_3$, 2.55 eV). The high E_T levels can effectively confine the triplet excitons in the phosphorescent emissive layer in the application of phosphorescent OLEDs as electron-transporting layer (ETL). The E_T value of p-PPtNN is a little smaller than that of p-PPtNT. It is also interpreted that the sp-hybrid cyano group in the *para*-orientation in p-PPtNN has a higher electron withdrawing ability and thus lowers the energy levels.

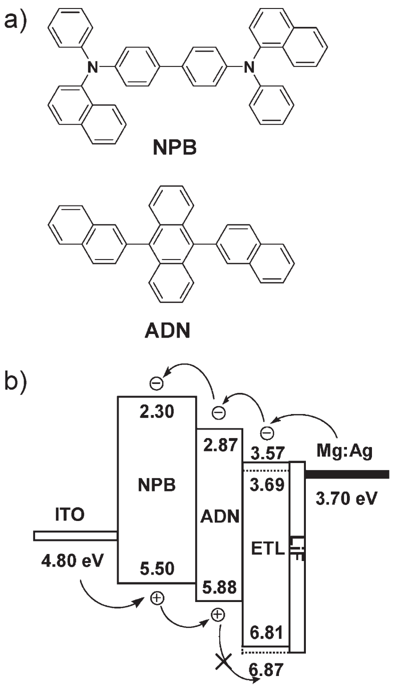

Figure 1. Chemical structures of the employed materials and energy level diagram for devices (The two pyridine compounds are used as ETL respectively). — p-PPtNT; ······ p-PPtNN

In comparison with green- and red-emitting OLEDs,[21,22] the performance of blue-emitting OLEDs is still lagging behind. In particular, there is still much room for improvement for both the efficiency and stability of deep-blue OLEDs. In this work, simple deep-blue OLEDs based on 9,10-di(2-naphthyl)anthracene (ADN) have been fabricated with a device structure as shown in Figure 1: indium-tin oxide (ITO)/α-napthylphenylbiphenyl diamine (NPB) [60 nm]/ADN [30 nm]/p-PPtNT or p-PPtNN [30 nm]/LiF [1 nm]/MgAg [100 nm 10: 1]. In the devices, ITO and the MgAg alloy were used as the anode and cathode, respectively. The organic layers included NPB as the hole-transporting layer, ADN as the light-emitting layer (LEL), and p-PPtNT or p-PPtNN as the ETL with a hole-blocking property to confine the emission zone in the ADN LEL.

Electroluminescent (EL) characteristics of the devices using the two pyridine compounds as the ETL are shown in Figure 2. The maximum current efficiencies of the devices based on p-PPtNT

Table 1. Spectroscopic and thermal data of the two pyridine compounds.

Compound	$T_d/T_m/T_g$ [a] [°C].	HOMO/LUMO energy level [eV]	$\lambda^{ab}_{max.}$[b] [nm]	$\lambda^{em.}_{max.}$[c] [nm]	E_T[d] [eV]
p-PPtNT	388/363/138.5	6.81/3.57	294/330	407	3.04
p-PPtNN	375/383/101.5	6.87/3.69	290/355	427	2.99

[a] T_d: decomposition temperature, T_m: melting point temperature, T_g: glass transition temperature. [b] λ^{ab}_{max}: maximum wavelength of absorption, measured in the solid film (vacuum deposited on quartz substrates. [c] λ^{em}_{max}: maximum wavelength of emission, measured in the solid film (vacuum deposited on quartz substrates). [d] E_T: triplet energy level.

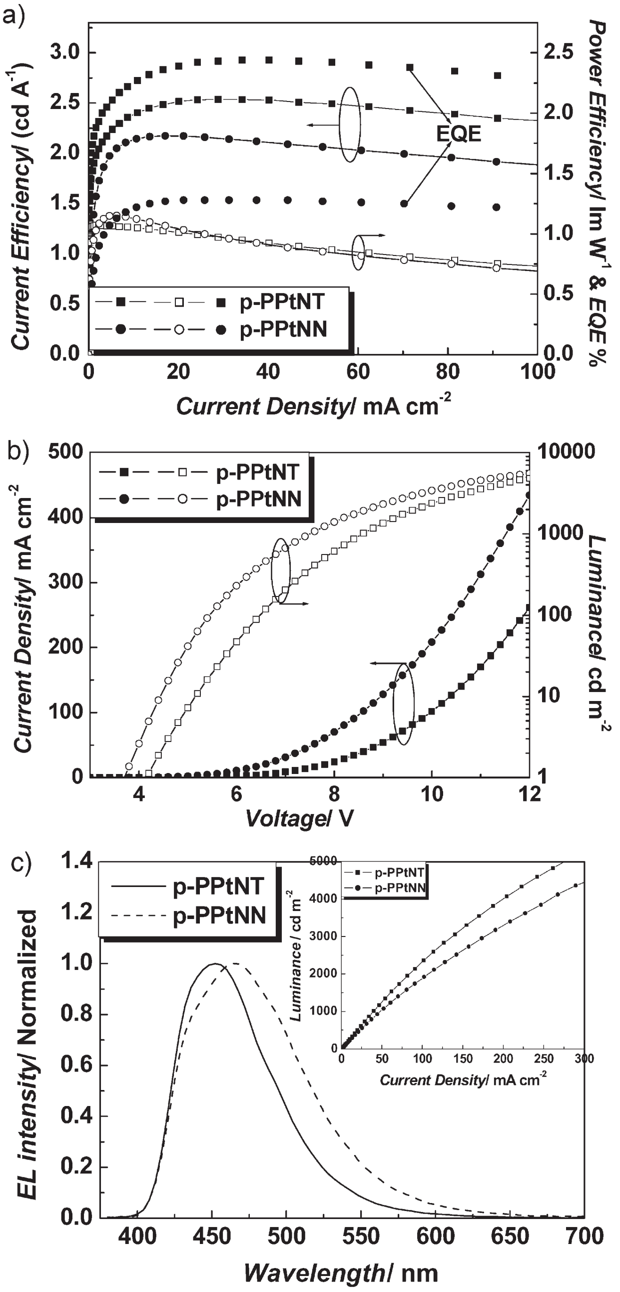

Figure 2. EL characteristics of devices using the new pyridine derivatives as ETL. Device structure: ITO/NPB (60 nm)/ADN (30 nm)/p-PPtNT or p-PPtNN (30 nm)/LiF (1nm)/MgAg (100 nm, 10: 1). a): Current efficiency (η_L)–current density (J)–power efficiency (η_P)–and EQE. b) J–voltage (V)–luminance (L). c) EL spectra, inset: L–J.

and p-PPtNN are 2.54 and 2.18 cd A^{-1}, respectively (Fig. 2a). These are considerably higher than the maximum current efficiencies of 1.6, 1.3, and 1.3 cd A^{-1} reported in the devices with similar structure, based on Alq$_3$ (as ETL), BCP (as hole-blocking layer)/Alq$_3$ (as ETL), and TPBI (as ETL), respectively.[23–28] In addition, the current efficiencies show only a mild decrease as the current density increases. For example, the device based on p-PPtNT exhibits a higher current efficiency of 2.51 cd A^{-1} at 20 mA cm^{-2} and a slightly lower current efficiency of 2.40 cd A^{-1} at 80 mA cm^{-2}. Compared with the device based on p-PPtNT, the current efficiency of the device based on p-PPtNN shows a little decrease. However, the value is still higher than the maximum current efficiencies of 1.6, 1.3, and 1.3 cd A^{-1} reported in the devices with similar structure, based on Alq$_3$ (as ETL), BCP (as hole-blocking layer)/Alq$_3$ (as ETL), and TPBI (as ETL), respectively.[23–28] The power efficiencies of the two devices are also higher than the values reported in the literature.[23–28] The external quantum efficiencies (EQEs) for the corresponding devices based on p-PPtNT and p-PPtNN are 2.44% and 1.28%, respectively (Fig. 2a). It is also noted that the EQEs show a mild decrease as the current density increases. The higher current and power efficiencies may be attributed to the lower LUMO energy levels, and good electron-transporting ability and hole-blocking ability of the two pyridine compounds. The lower LUMO energy levels facilitate electron injection from the cathode to the organic layer, while the good electron-transporting ability and hole-blocking ability can jointly assure electron charge balance. The efficiencies of the device based on p-PPtNT are higher than that of the device based on p-PPtNN, possibly because of a better electron-transporting ability.

As shown in Figure 2b, the devices have low turn-on voltages (defined as the voltage at a luminance of 1 cd m^{-2}) of 4.1 V (p-PPtNT) and 3.7 V (p-PPtNN) in comparison with those of devices based on Alq$_3$ (as ETL), BCP (as hole-blocking layer)/Alq$_3$ (as ETL), and TPBI (as ETL).[23–28] It is considered that the smaller turn-on voltages are attributed to the lower LUMO energy levels of the two pyridine compounds, which facilitates electron injection from the cathode to the organic layer. Moreover, besides the turn-on voltage, the driving voltage of the device based on p-PPtNN is smaller than that of the device based on p-PPtNT. For instance, the driving voltages for p-PPtNN are only 8.6 and 9.9 V at 100 and 200 mA cm^{-2}, while those for p-PPtNT are 10.0 and 11.4 V, respectively. The smaller driving voltage and turn-on voltage are closely related to the lower LUMO energy level of p-PPtNN.

Figure 2c shows the EL spectra and luminance (L)–current density (J) characteristics of the devices based on the two pyridine compounds. The EL peak positions (and Commission Internationale de L'Eclairage (CIE) coordinates) of the devices based on p-PPtNT and p-PPtNN are 452 nm (0.15, 0.12) and 464 nm (0.16, 0.20), respectively. It should also be pointed out that the full widths at half-maximum (λ_{FWHM}) for the two devices are 73 and 94 nm, respectively. The CIE coordinates and narrower λ_{FWHM} of the device based on p-PPtNT show a color purity considerably better than reported for a Alq$_3$-based device (CIE 0.17, 0.17).[23–28] Deep-blue emission of the device based on p-PPtNT should be attributed to the electroluminescence of ADN. The better color purity is attributed to the good hole-blocking property of the pyridine derivatives, which helps to confine the emission zone in the ADN layer. The λ_{FWHM} for the device based on p-PPtNN is obviously broader than that for p-PPtNT. It may be attributed to the formation of an exciplex in the ADN/p-PPtNN interface, which can induce a red-shift on account of the more electron-deficient molecular structure of p-PPtNN. In addition, the L–J curve of the device based on p-PPtNT is above that of the device based on p-PPtNN (the inset in Fig. 2c). The formation of an exciplex in the ADN/p-PPtNN interface can also take charge of the weaker luminance of the device based on p-PPtNN. This is another possible reason for the lower efficiencies of the device based on p-PPtNN compared to that of the device based on p-PPtNT (Fig. 2a).

To summarize, two multiaryl-substituted pyridine derivatives, namely p-PPtNT and p-PPtNN, have been synthesized and applied as ETMs with good hole-blocking ability in high-performance deep-blue OLEDs. The maximum current efficiency of the devices based on the new compounds is above 2.1 cd A^{-1}, which is over 70% higher than for previously reported devices using Alq_3 and TPBI instead. The CIE coordinates of the device based on p-PPtNT are close to the National Television System Committee (NTSC) standards of 0.14, 0.08[29] for blue emission.

Experimental

The chemical structures and synthetic routes towards p-PPtNT and p-PPtNN are shown in Scheme 1. They were prepared using methods similar to those described in the literature [15–17]. Taking p-PPtNN as an example, 1,4-diacetylbene (1.62 g, 10 mmol) was first added to an alcohol solution (50 mL) of *p*-methyl benzaldehyde (3.00 g, 25 mmol) under stirring. A 10% NaOH solution (10 mL) was then dropped into the alcohol solution under rapid stirring [15]. Stirring was continued for another 12 h. The precipitate then was collected, washed with H_2O, and recrystallized from alcohol. Yellow acicular crystals (p-PPtNN I) (3.2 g, 80% yield) were collected. The crystalline p-PPtNN I (1.83 g, 5 mmol), benzoylacetonitrile (1.45 g, 10 mmol), and anhydrous ammonium acetate (1 g) were added into a three-necked flask [17]. Glacial acetic acid (50 mL) was then injected in under a nitrogen atmosphere. The mixture was refluxed for 24 h under stirring. The whole process was completed under a nitrogen atmosphere. After cooling to room temperature, the reaction mixture was filtered. A pale yellow powder was recrystallized from 1,2-diclorobenzene. A white solid of p-PPtNN was obtained. p-PPtNT were recrystallized with the same solvent.

OLEDs were fabricated on patterned ITO-coated glass substrates with a sheet resistance of $30\,\Omega/\square$. The substrates were cleaned with Decon 90, rinsed in de-ionized water, dried in an oven, and finally exposed to UV-ozone for about 25 min. The ITO substrates were then immediately transferred into a deposition chamber with a base pressure of 1×10^{-6} mbar. Organic layers were sequentially deposited at a rate of $0.1 \sim 0.2$ nm s^{-1} by conventional vapor vacuum deposition. The MgAg alloy was then prepared by co-evaporation of Mg and Ag at a volume ratio of 10:1 after LiF of 1 nm was deposited.

4,4′-(1,4-Phenylene)bis(2-phenyl-6-p-tolylnicotinonitrile) (p-PPtNT): ^{1}H NMR (400 MHz, $CDCl_3$, δ): 8.14 (d, $J = 8.16$ Hz, 4H), 8.08–8.05 (m, 4H), 7.90 (s, 2H), 7.88 (s, 4H), 7.58–7.56 (m, 6H), 7.35 (d, J = 8.08 Hz, 4H), 2.44 (s, 6H); ^{13}C NMR (400 MHz, $CDCl_3$, δ): 162.6, 159.6, 154.4, 141.3, 138.4, 138.2, 134.7, 130.3, 130.0, 129.6, 128.7, 127.7, 118.4, 118.0, 103.9, 21.6. HRMS (EI, *m*/*z*): $[M]^+$ calcd. for $C_{44}H_{30}N_4$: 614.25; found, 614.2466. Anal. calcd. for $C_{44}H_{30}N_4$: C 85.97, H 4.92, N 9.11; found: C 83.56, H 4.497, N 8.671.

6,6′-(1,4-Phenylene)bis(2-phenyl-4-p-tolylnicotinonitrile) (p-PPtNN): ^{1}H NMR (400 MHz, $CDCl_3$, δ): 8.32 (s, 4H), 8.06–8.04 (m, 4H), 7.87 (s, 2H), 7.62 (d, $J = 8.08$ Hz), 7.59–7.51 (m, 6H), 7.40 (d, $J = 7.88$ Hz, 4H), 2.47 (s, 6H); HRMS (EI, *m*/*z*): $[M]^+$ calcd. for $C_{44}H_{30}N_4$: 614.25; found, 614.2466. Anal. calcd. for $C_{44}H_{30}N_4$: C 85.97, H 4.92, N 9.11; found: C 85.78, H 4.727, N 9.473.

Acknowledgements

The authors thank the Center of Super-Diamond and Advanced Film (COSDAF), Department of Physics and Materials Science, City University of Hong Kong. This work is financially supported by the National Natural Science Foundation of China (Grant No. 60118033), the National High Technology Research and Development Program of China (863 Program) (Grant No. 2008AA03A327), the National Basic Research Development Program of China (973 Program) (Grant No. 2006CB933000), the Croucher Foundation of Hong Kong, and RGC of Hong Kong (Grant No: CityU 101508). Supporting Information is available online from Wiley InterScience or from the author.

Received: July 21, 2009
Published online: October 13, 2009

[1] C. W. Tang, S. A. Vanslyke, *Appl. Phys. Lett.* **1987**, *51*, 913.
[2] C. Hosokawa, H. Higashi, N. Nakamura, T. Kusumoto, *Appl. Phys. Lett.* **1995**, *67*, 3853.
[3] T. Noda, H. Ogawa, N. Noma, Y. Shirota, *Adv. Mater.* **1997**, *9*, 720.
[4] K. Tamao, M. Uchida, T. Izumizawa, K. Fukukawa, S. Yamaguchi, *J. Am. Chem. Soc.* **1998**, *120*, 9714.
[5] C. H. Chen, J. Shi, *Coord. Chem. Rev.* **1998**, *171*, 161.
[6] V. A. Montes, R. Pohl, J. Shinar, P. Anzenbacher Jr. *Chem. Eur. J.* **2006**, *12*, 4523.
[7] H. H. Fong, W. C. H. Choy, K. N. Hui, Y. J. Liang, *Appl. Phys. Lett.* **2006**, *88*, 113 510.
[8] H. Inomata, K. Goushi, T. Masuko, T. Konno, T. Imai, H. Sasabe, J. J. Brown, C. Adachi, *Chem. Mater.* **2004**, *16*, 1285.
[9] L. S. Hung, C. H. Chen, *Mater. Sci. Eng. R* **2002**, *39*, 143.
[10] M. Nomura, Y. Shibasaki, M. Ueda, K. Tugita, M. Ichikawa, Y. Taniguchi, *Synth. Met.* **2000**, *122*, 1832.
[11] Y. Sakamoto, T. Suzuki, A. Miura, H. Fujikawa, S. Tokito, Y. Taga, *J. Am. Chem. Soc.* **2003**, *125*, 7166.
[12] S. J. Su, T. Chiba, T. Takeda, J. Kido, *Adv. Mater.* **2008**, *20*, 2125.
[13] S. J. Su, D. TanaKa, Y. J. Li, H. Sasabe, T. Takeda, J. Kido, *Org. Lett.* **2008**, *10*, 941.
[14] H. Sasabe, E. Gonmori, T. Chiba, Y. Li, D. Tanaka, S. J. Su, T. Takeda, Y. Pu, K. Nakayama, J. Kido, *Chem. Mater.* **2008**, *20*, 5951.
[15] A. Khatyr, H. Maas, G. Calzaferri, *J. Org. Chem.* **2002**, *67*, 6705.
[16] D. C. G. A. Pinto, A. M. S. Silva, J. A. S. Cavaleiro, J. Elguero, *Eur. J. Org. Chem.* **2003**, 747.
[17] a) S. Marchalin, J. Kuthan, *Collection Czechoslovak Chem. Commun.* **1985**, *50*, 1862. b) S. Marchalin, J. Kuthan, *Collection Czechoslovak Chem. Commun.* **1985**, *50*, 1870. c) S. Marchalin, J. Kuthan, *Collection Czechoslovak Chem. Commun.* **1985**, *50*, 1962.
[18] H. Xin, F. Y. Li, M. Shi, Z. Q. Bian, C. H. Huang, *J. Am. Chem. Soc.* **2003**, *125*, 7166.
[19] S. C. Lo, N. A. H. Male, J. P. J. Markham, S. W. Magennis, P. L. Burn, O. V. Salata, I. D. W. Samuel, *Adv. Mater.* **2002**, *14*, 975.
[20] Q. X. Tong, S. L. Lai, M. Y. Chan, Y. C. Zhou, H. L. Kwong, C. S. Lee, S. T. Lee, *Chem. Phys. Lett.* **2008**, *455*, 71.
[21] P. F. Wang, Z. Y. Xie, S. W. Tong, O. Y. Wong, C. S. Lee, N. B. Wong, L. S. Hung, S. T. Lee, *Chem. Mater.* **2003**, *15*, 1913.
[22] J. Y. Li, D. Liu, Z. R. Hong, S. W. Tong, P. F. Wang, C. W. Ma, O. Lengyel, C. S. Lee, H. L. Kwong, S. T. Lee, *Chem. Mater.* **2003**, *15*, 1486.
[23] Y. Q. Li, M. K. Fang, Z. Y. Xie, S. T. Lee, L. S. Hong, J. M. Shi, *Adv. Mater.* **2002**, *14*, 1317.
[24] C. H. Liao, M. T. Lee, C. H. Tsai, C. H. Chen, *Appl. Phys. Lett.* **2005**, *86*, 203 507.
[25] X. Y. Jiang, Z. L. Zhang, W. Q. Zhu, S. H. Xu, *Displays* **2006**, *27*, 161.
[26] J. M. Shi, C. Tang, *Appl. Phys. Lett.* **2002**, *80*, 3201.
[27] T. H. Liu, W. J. Shen, C. K. Yen, C. Y. Iou, H. H. Chen, B. Banumathy, C. H. Chen, *Synth. Met.* **2003**, *137*, 1033.
[28] W. J. Shen, R. Dodda, C. C. Wu, F. I. Wu, T. H. Liu, H. H. Chen, C. H. Chen, C. F. Shu, *Chem. Mater.* **2004**, *16*, 930.
[29] G. Rajeswaran, M. Itoh, M. Boroson, S. Barry, T. K. Hatwar, K. B. Kahen, K. Yoneda, R. Yokoyama, T. Yamada, N. Komiya, H. Kanno, H. Takahashi, *SLD'00 Digest* **2000**, *40*, 1.